Design of STF phase-2 accelerator beam line

Ilmoon Hwang*

Department of Physics, Kyoungpook National University,

SanKyeok-dong 1370, Buk-gu, Daegu, 702-701, Korea

(Dated: December 11, 2008)

Abstract

The design of low emittance beam generation from L-band RF gun and beam transmission to optical cavity for high brightness X-ray generation, and the design of high charge transmission from L-band RF gun through ILC cryomodule for various beam test of ILC cryomodule are summarized in this report. The optimization of the beam line of STF phase-2 accelerator is, at first, performed for ILC beam of high bunch charge case using program 'PARMELA'. Then, it is checked for low bunch charge case of high brightness X-ray generation. The design was confirmed for reasonable low emittance beam for ILC case, and very low emittance beam generation for compact X-ray source accelerator case.

*Electronic address: imhwang@postech.ac.kr,imhwang@knu.ac.kr

I. INTORDUCTION

The superconducting RF test facility (STF) in KEK is aiming to promote R&D of superconducting linear accelerator to be used in the International Linear Collider (ILC)[1, 2]. The STF construction is planned to have two stages, such as phase-1 plan and phase-2 plan. The phase-1 plan is aiming to have quick experience on all aspect of 1.3GHz SC cavity and cryomodule technologies, as well as to construct new cavity surface treatment facilities, such as electro-chemical polishing and clean room to get stable high gradient performance. The developments of the phase-2 are started in 2008 to construct one ILC main linac RF unit to demonstrate ILC accelerator performance and production capability. The phase-2 accelerator will install ILC beam produced by normal-conducting RF gun of L-band frequency. It is photocathode RF gun irradiated by UV multibunch laser lights. In the intermediate stage of construction, STF accelerator will be installed the high brightness X-ray generation function in parallel. The beam line design should satisfy the both beam function with the same beam line configuration.

II. BEAM-OPERATION MODE AND BEAM-LINE CONFIGURATION

The ILC polarized electron source must produce 2625 bunches of 2.0×10^{10} electrons at 5 Hz with polarization greater than 80%[1]. The electron bunch is produced by a laser illuminating a photocathode in a DC gun and its length is compressed down to about 20ps FWHM by the bunching system. The buncher has 5 cells with $\beta = 0.75$ and a gradient of 5.5MVm and is followed by a 660G solenoid field to focus the beam. Two 50 cell normal conducting TW accelerating sections at a gradient of 8.5MVm increase the beam energy to 76MeV. The vertical chicane provides energy collimation and several diagnostic devices are placed before injection into the Super Conducting (SC) booster linac.

In STF phase-2, an L-band RF gun with Ce-Te cathode and two capture cavities consisting of 9-cell SC cavities are adopted in contrast with the original RDR. The schematic beam-line configurations are described in Figure 1. The capture cavities are placed in the same cross-sectional configuration of the STF cryomodule with short length. Several focusing quadrupoles and diagnostic devices are followed in front of the main linac. For this configuration, a round beam with 3.2nC charge and 20ps length is considered in our pre-

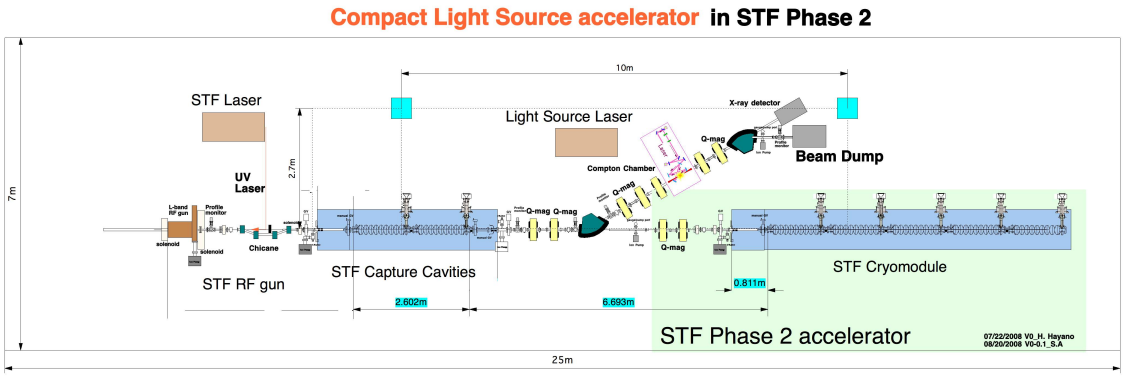

FIG. 1: Schematic drawing of STF Phase-2.

liminary design. The normalized transverse emittance is expected below 20μmrad. Another option with 1.0nC charge is prepared for future undulator test. The beam loading, the control of LLRF and the damping performance of of HOM excited by the beam will be tested also using these high charge beams.

Additional operation mode can be selected by a bending magnet shown in middle of Figure 1. It provides X-ray source by Compton scattering with optical cavity laser for medical and material science. A beam of 0.1 nC charge with 1μmrad is desirable.

III. DESIGN SETUP FOR BEAM TRANSPORTATION

The fields of STF RF gun and STF capture cavities were obtained by POISSON/ SUPERFISH developed by the Los Alamos Accelerator Code Group. The beam dynamics code PARMELA supplied by the same group was used to calculate the beam parameters by tracking the macro-particles. The program setup and the design process will be described in the following subsections.

A. Design components for PARMELA

PARMELA simulation was performed with the simplified structure as shown in Figure 2. The cathode surface is set to zero position in longitudinal direction and the field of the RF gun is calculated up to 32.5cm. After a travel of 3.5m drift, a beam enters the capture cavities. Final beam properties are calculated at 1m downstream from the capture cavities.

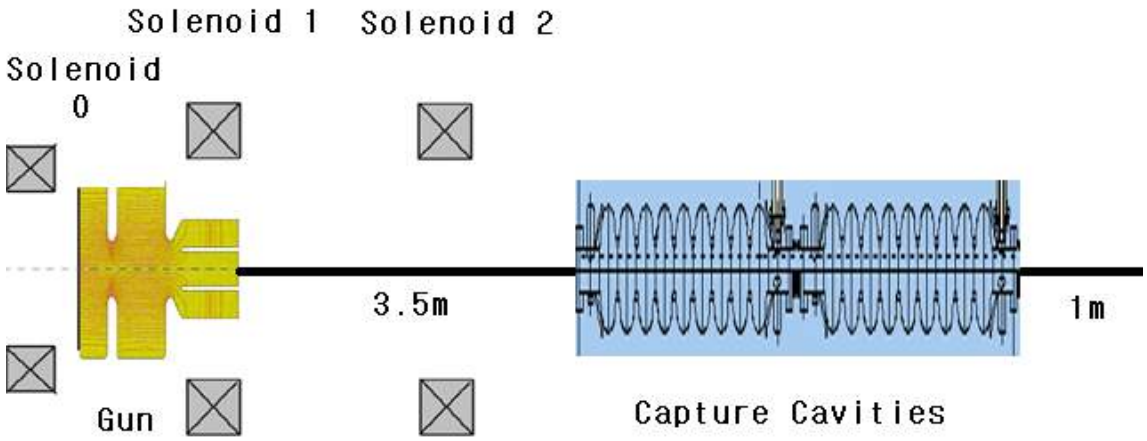

FIG. 2: Components of PARMELA simulation.

B. Initial distribution of electron bunch

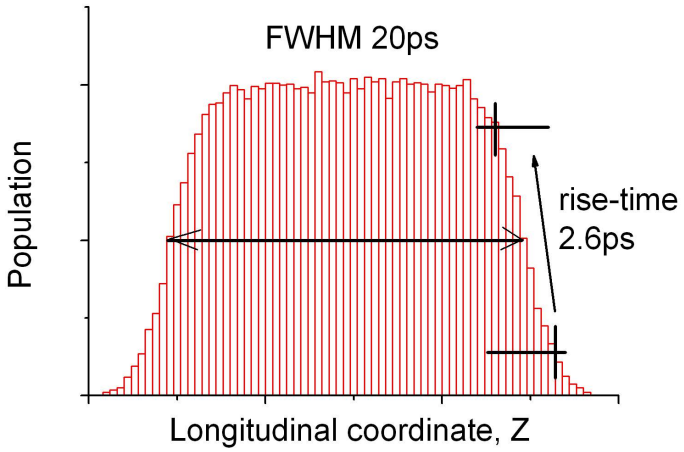

FIG. 3: Longitudinal distribution of pulse.

The laser pulse is assumed as 'beer-can' which is round in transverse direction and has hard edges. The electron bunch has the same shape and the Gaussian distributed momentum in transverse direction. The initial transverse emittance is assumed as 0.42μmrad per 1mm laser radius[3, 4]. When electrons emit by a laser pulse, the energy distribution of the emitted electron depends on the cathode material and the photon energy. Cs-Te and 266nm wavelength are accounted and the kinetic energies of all electrons are assumed as 0.55eV for simplicity[3]. The longitudinal distribution of the electron bunch affects on the transverse

emittance. A flat-top pulse shows smaller emittance than a single Gaussian pulse. An ellipsoidal shape is better than a flat-top but requires complex laser system[5–8]. A flat-top made by addition of 8 Gaussian pulses is used in this report. It has 20ps FWHM and 2.6ps rise-time from 10% to 90%.

1. *Random number*

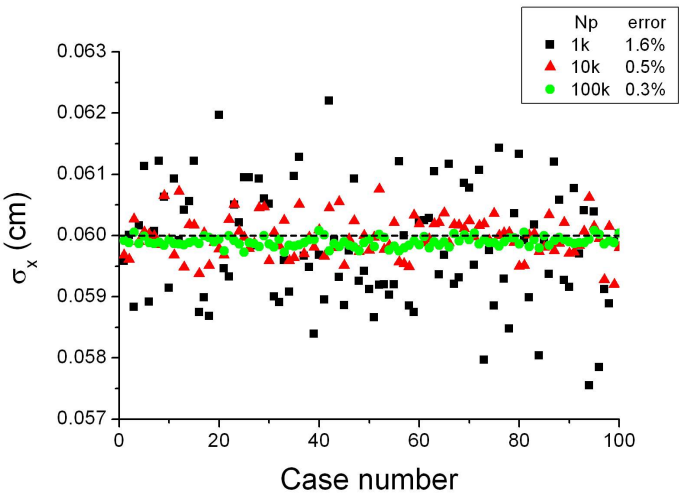

FIG. 4: Deviation of beam size.

The electron bunch is described by the macro-particles with the random numbers. Many macro-particles are needed for accurate calculation but require high computing power. Examples are shown in Figure 4 to presume the error level. Transverse sizes with various random-number seed are calculated when the number of the macro-particle are 1,000, 10,000 and 100,000. 0.5% accuracy is expected with 10,000 macro-particles in the emittance calculation.

2. *Sobol's sequence*

A random sequence should be statistically uncorrelated in all measurable respects. The random number used in the computer simulation is not real 'random', but the computer-generated sequences termed "pseudo-random". Many algorithms are used to enhance the

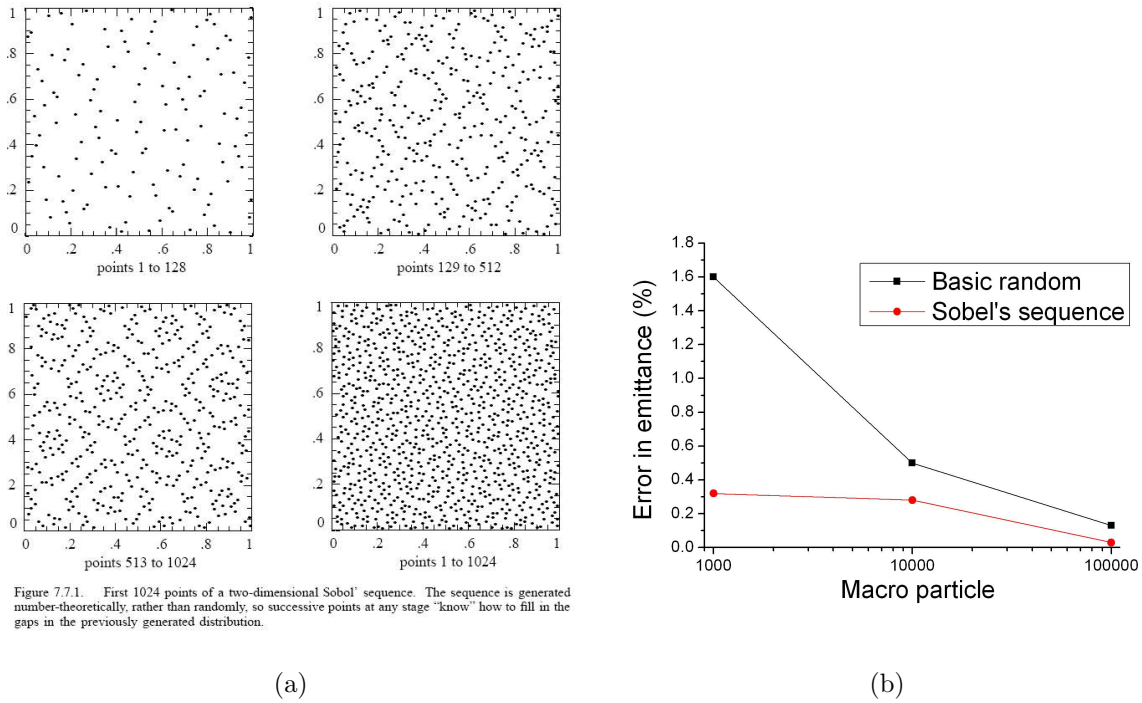

FIG. 5: (a) Example of Sobol's sequence[9] and (b) convergence comparison.

randomness of the computer random. To avoid an unphysical error caused by a numerical reason, the randomness and many macro-particles are essential. An error decreases as $1/\sqrt{N_P}$. It requires a heavy computing power to reduce a numerical error. Therefore several 'quasi-random' algorithms are used for run-time saving, even if the randomness is sacrificed. Sobol's sequence[9] is used for an initial electron state with 2,000 macro-particles in this report. It has a complex pattern as in Figure 5(a), and small error in initial distribution as in Figure 5(b).

C. RF gun

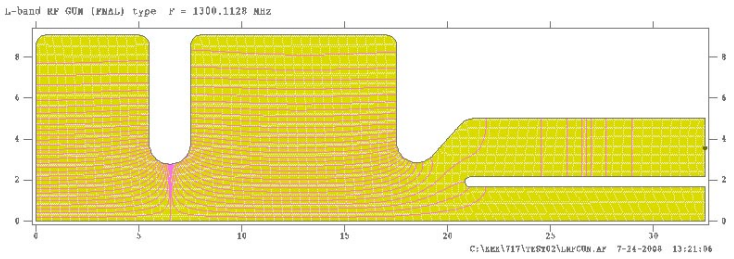

FIG. 6: Structure of L-band RF gun.

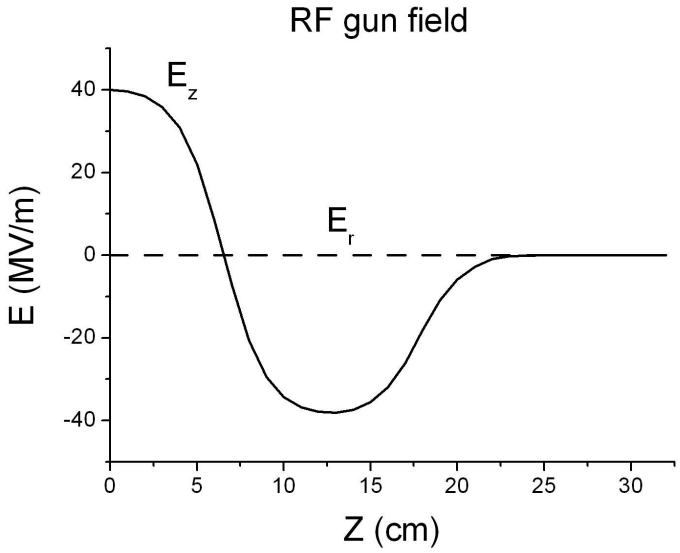

FIG. 7: Electric field of RF gun.

The TESLA Test Facility (TTF) is operated by the photoinjector including an RF gun at 1.3GHz[10]. A laser pulse strikes the cathode surface normally while the electron beam gets out of the straight way by a four-dipole chicane. As shown in Figure 6, the L-band RF gun is 1 and 1/2-cell with a Cs-Te cathode and typically designed for sub μmrad transverse emittance with nC charge per bunch[11]. The field calculating range for the RF gun is up to 32.5cm longitudinally and 9cm transversely. The numbers of the grids are 200 longitudinally and 20 transversely. The transverse coordinates are limited by the wall of the RF gun mainly at iris 2.78cm and near exit 1.675cm. It is enough but the PARMELA does not check it. The maximum peak field at the cathode surface is assumed as 40MV/m which is provided by 3MW klystron. There is no transverse electric field as shown in Figure 7.

D. Solenoid

After a photo-emission on the cathode, an electron beam diverges by a space-charge force. Each part of the beam feels different force. For example, the center of the bunch repels stronger than the edge. Therefore, the distribution in the phase space broadens and the transverse emittance increases. A solenoid field can focus the diverging beam by a kick proportional to offset. The solenoid field makes the beam focus and the broadening

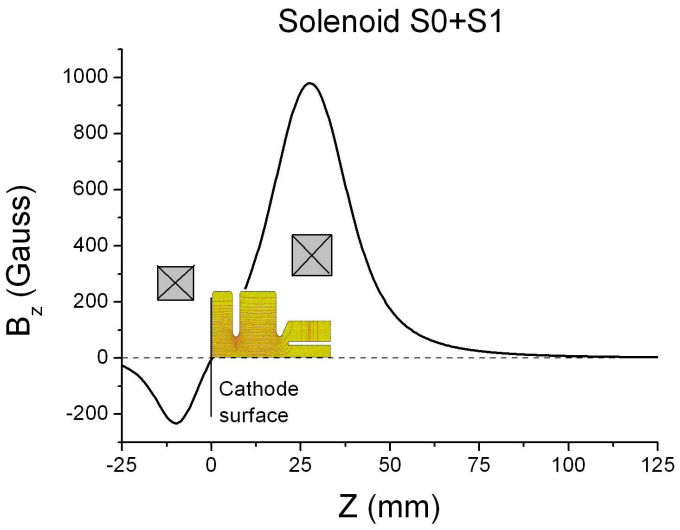

FIG. 8: Solenoid configuration and field.

in the phase space can be recovered after a certain drift space. It called the emittance compensation process[12]. The main solenoid is placed close to the cathode and a smaller solenoid is located behind the cathode for zero magnetic field on the cathode surface as shown in Figure 8. The position and the strength are assigned by the reference of Photo Injector Test facility at Zeuthen (PITZ)[13, 14]. The main solenoid is 12cm long, 14cm radius and placed at 27.5cm. It is approximated by 7 rings in PARMELA.

E. Capture cavity

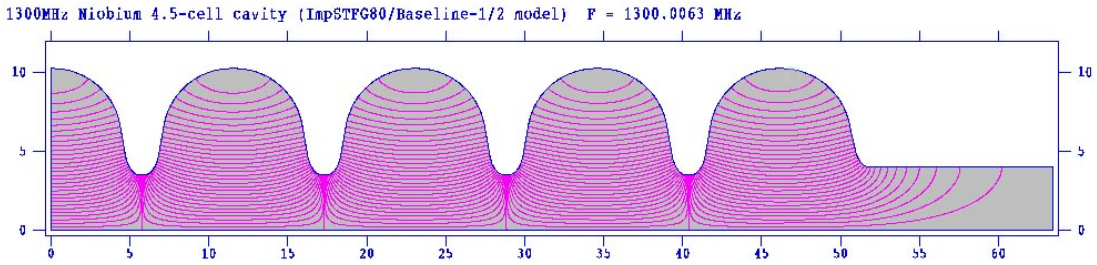

FIG. 9: Half of capture cavity.

An electron beam generated at the RF gun travels a drift space and enters into the capture cavities which are two niobium 9-cell cavities operating at 1.3GHz[15]. These cavities are

called 'booster cavities' also. Each cavity is 1269.224mm long and a standing wave structure as shown in Figure 9[11]. The distance of the couplers is 1337mm. The accelerating gradient of these capture cavities are usually limited to small value in order to prevent the edge effect when a low energy beam like as 4MeV is injected. 12MV/m is selected according to the TTF[8, 13, 16–18]. In the TTF design, a TESLA module with eight 9-cell superconducting 1.3GHz cavities boosts the beam to 127MeV. The gradient of the first four cavities is chosen as 12MV/m and next four cavities are set to 20MV/m roughly. Note that the number of the mesh should be the same as the RF gun in the PARMELA.

IV. DESIGN PROCEDURE FOR BEAM TRANSPORTATION

The beam line is designed for three cases with the same configurating that is described in the previous section. At first, the ILC setup with a 3.2nC charge, 20ps length and round beam is examined. The smaller charge of 1nC for STF undulator test is the next. A beam of 0.1nC is used for X-ray source by Compton scattering for the third examination.

As the first step, the RF gun and solenoids are investigated, then the capture cavities are considered. The peak electric field on the cathode surface is fixed to 40MV/m but the phase of the RF gun is surveyed. The shape of main solenoid is fixed but the solenoid strength is varied and is represented by the peak field strength. The bucking solenoid is assumed as 3cm long, 10cm radius and placed at 9.5cm behind the cathode surface. 7 rings are used for the field calculation. The bucking solenoid makes the magnetic field on the cathode zero. An additional solenoid which has varying strength and the same shape with the first main one is considered in order to overcome a long drift between the RF gun and the capture cavities. The position of the second solenoid is tested at 2m and 2.5m. The field gradients of the capture cavities are selected as 12MV/m to avoid strong focusing and the phases of each cavities are changed separately. This process is repeated for each parameter case with the same setup and the geometry.

A. 3.2nC

The initial electron beam has 3.2nC charge, a flat-top temporal shape with 20ps length and 3mm radius corresponding to 1.5mm standard deviation.

1. *Gun, Solenoid and 2m drift*

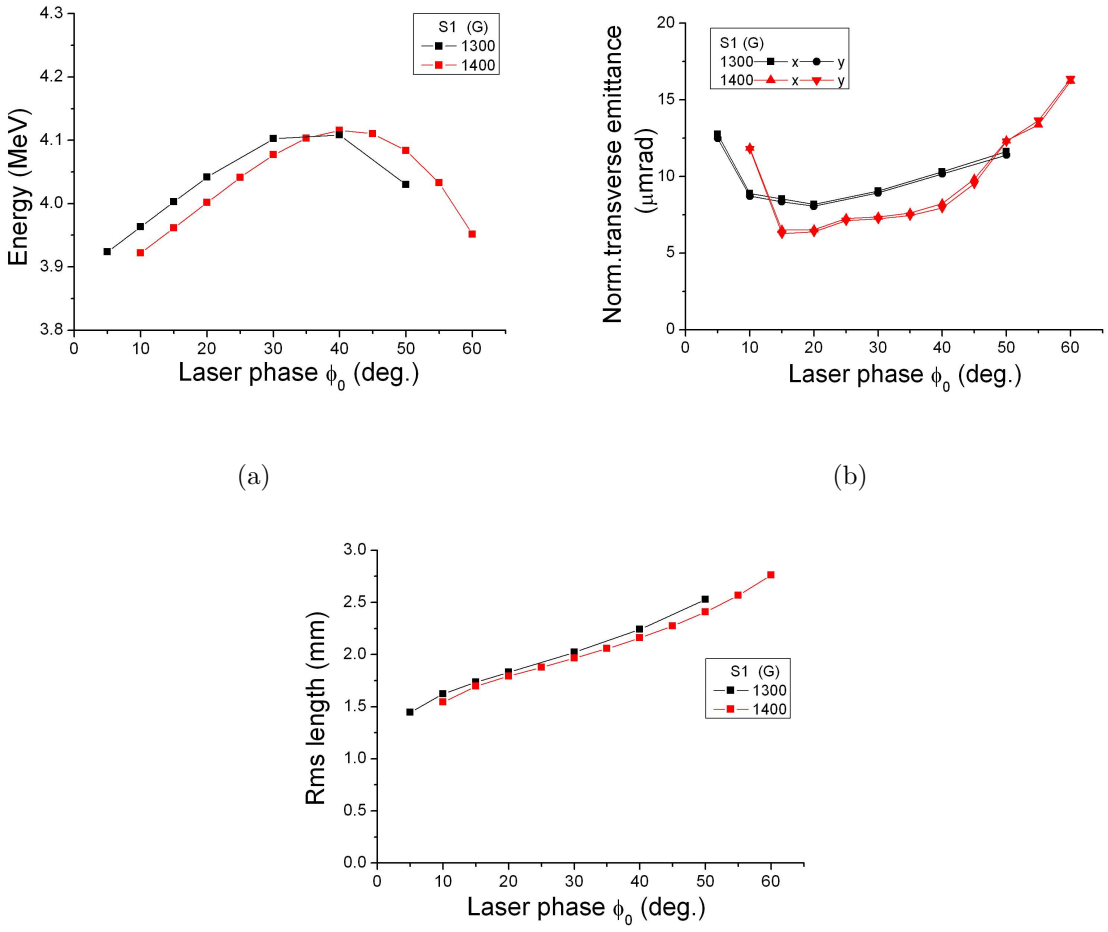

(a) (b)

(c)

FIG. 10: Laser phase dependency of (a) beam energy, (b) emittance and (c) bunch length at gun exit.

The RF gun and solenoids are investigated with the observation point at 2m downstream of the drift space. The emittance compensating process looks good at 1300G or 1400G of the peak solenoid field. These solenoid strength are tested with the laser phase change. As shown in Figure 10(a), the maximum energy is obtained near 35°. No electron can be emitted below zero phase because the phase is defined as *sin* form. If an electron is emitted near 90°, the extracting field is maximized but the electron cannot move to the next cell of the RF gun due to slow speed and becomes out of phase. The transverse emittance can be below 10μmrad between 20° and 40° as shown in Figure 10(b). The bunch length

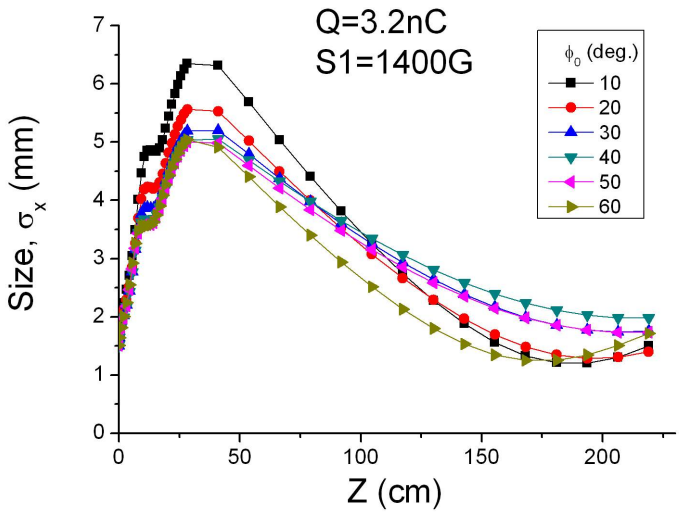

FIG. 11: Evolution of beam size.

increases monotonously with the phase as shown in Figure 10(c). The laser phase is selected as 33° which is a middle value between the energy maximum and the transverse emittance minimum.

2. 3.5m drift

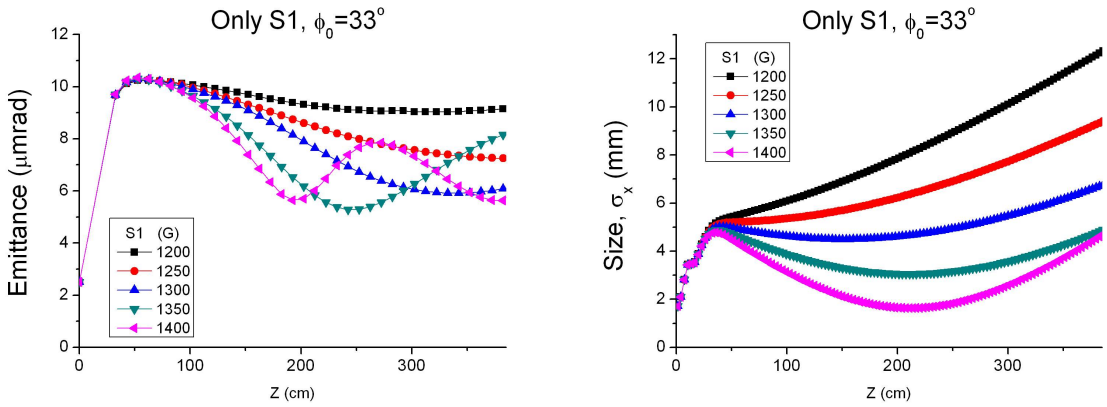

(a) (b)

FIG. 12: Evolution of (a) emittance and (b) beam size after 3.5m drift.

A drift after the RF gun and the solenoid is required for the emittance compensating

process and a long drift space is desirable for the laser injection path and the beam diagnostics. 3.5m drift is recommended but there is a problem. It is too long for the emittance compensating process. The evolution of the transverse emittance and the transverse size with various solenoid field are shown in Figure 12. The emittance is compensated above 1200G and minimized at 2.2m with 1350G. Double minimun appears at 1400G. It is caused by a misalignment of the phase-space distribution of the longitudinal slice. The entrance of the capture cavity should be placed at minimum size point but no case can be minimized at the end of 3.5m drift as shown in Figure 12(b). That is a reason to require the second solenoid in the drift space.

3. Additional solenoid at 2m

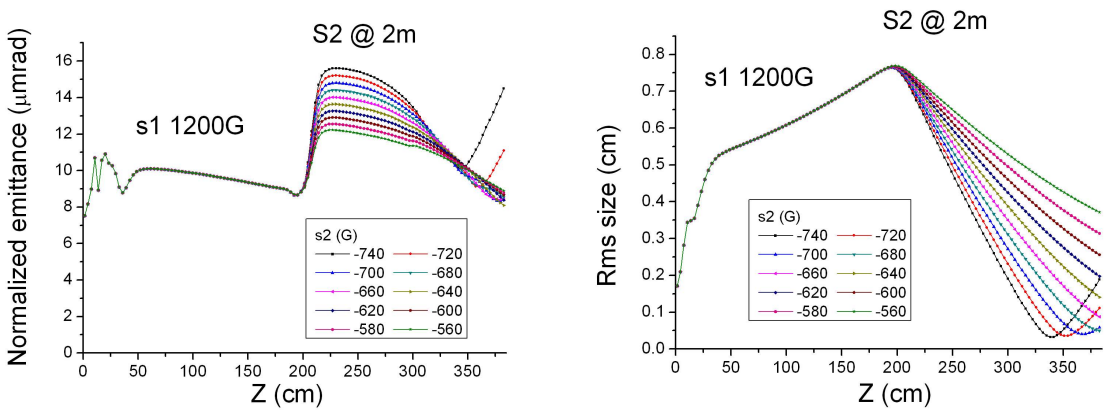

(a) (b)

FIG. 13: Evolution of (a) emittance and (b) beam size with second solenoid located at 2m.

As the first try, the second solenoid is placed at 2m down downstream from the cathode surface of the gun. It is just before the minimum size point. Actually, this position is not good to accelerate the beam according to Ferrario's working point[12]. In the transverse emittance compensating procedure, the first solenoid should be located close to the cathode in order to focus the divergent beam dut to space-charge force. After the solenoid, the focused beam passes a minimum or two local minimum, then the beam spreads out. The accelerating cavity should be placed near minimum. Otherwise, the transverse emittance increases at the second solenoid position as shown in Figure 13(a). The strengths of the

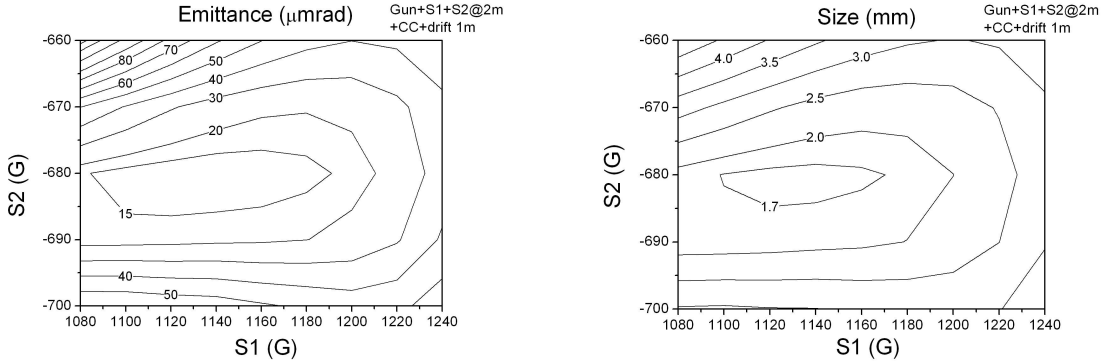

(a) (b)

FIG. 14: (a) Emittance and (b) beam-size map with solenoid scan when the second solenoid located at 2m.

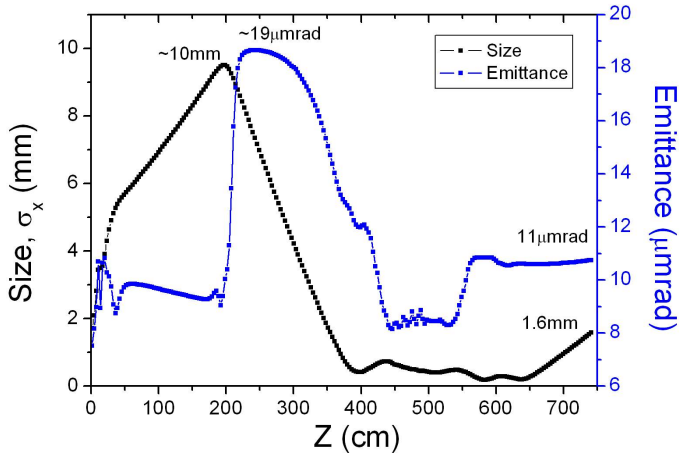

FIG. 15: Optimal case when second solenoid located at 2m.

solenoids are chosen to avoid large size at the entrance of the capture cavity. The rms beam size of typical comibinations are shown in Figure 13(b). The size reaches 0.7cm at the second solenoid and decreases. When strong field like as 740G is applied, the focusing is too strong, then the beam size reduced to 5mm. Due to small size the space-charge effect is dominant again, therefore the beam becomes divergent and the emittance increases. The second solenoid should be adjusted to avoid this expansion. In brief, the key point is size control. The beam do not strike the wall and avoid strong space-charge effect. The map of two solenoids scan is helpful to select a working point. While the size is kept small as

shown in Figure 14(b), the transverse emittance is near minimum as shown in Figure 14(a). With the capture cavities, the optimized case shows 11μmrad emittance in Figure 15. The configuration of the capture cavities will be explained in the next case.

4. Additional solenoid at 2.5m

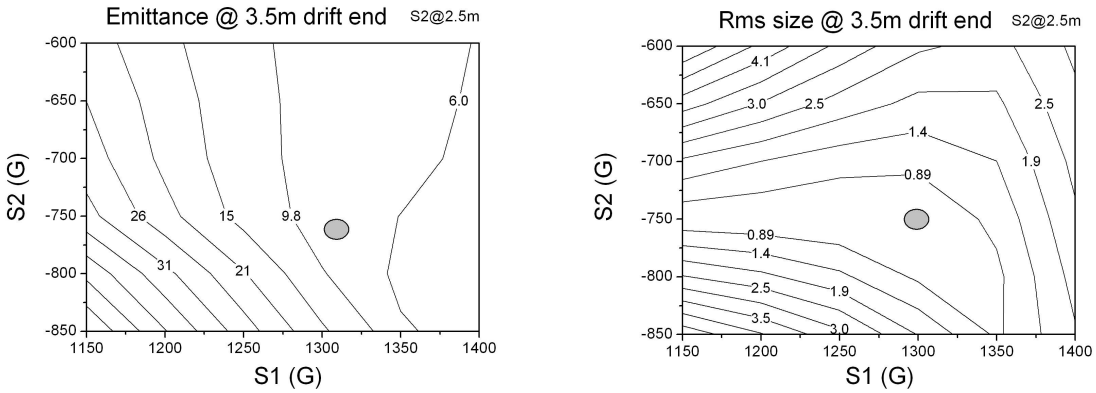

(a) (b)

FIG. 16: (a) Emittance and (b) beam-size map with solenoid scan when the second solenoid located at 2.5m.

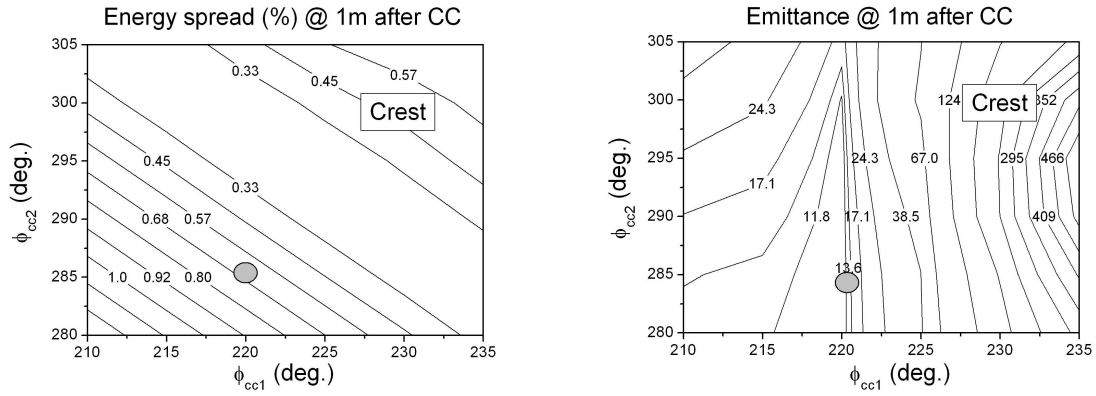

(a) (b)

FIG. 17: (a) Energy spread and (b) emittance map with cavity phase when the second solenoid located at 2.5m.

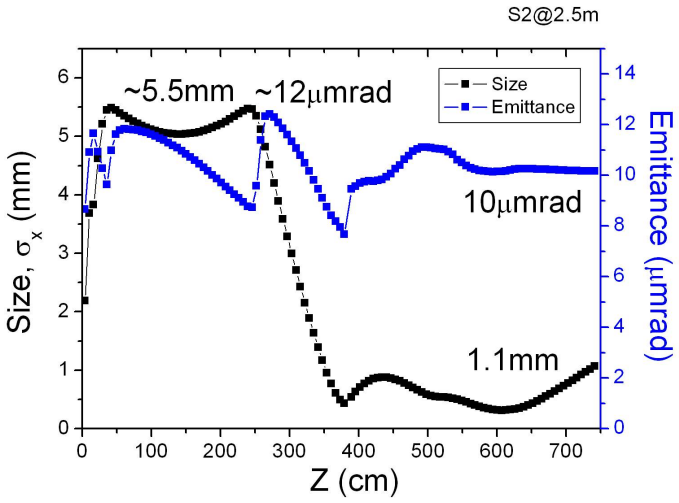

FIG. 18: Optimal case when second solenoid located at 2.5m.

If the second solenoid is located at 2m, there is an emittance expansion. When the second solenoid is placed at 2.5m, the beam is accelerated after the size minimum. The strength of the solenoids are selected from the scan map in the same way. The size is near the minimum as shown in Figure 16(b), then the emittance is about 10μmrad as shown in Figure 16(a). The selection of the solenoid strength is marked by the grey filled circle. The amplitudes of the capture cavities are fixed as 12MV/m which should be test later. The phases of the capture cavities are selected in the scan map. The emittance, the size, the energy gain and the energy spread are considered. The energy gain is maximized at the crest. The crest of the acceleration is at the phases of 230° for the first cavity and 301° for the second one. At the same time, the energy spread is minimized as shown in Figure 17(a). The beam becomes longer and the emittance compensation is not optimized. If the phases are selected as the grey circles shown in Figure 17(b), the bunch lengthening is suppressed and the emittance is about 10μmrad while the energy spread becomes a little large. Comparing with 2m case, the final emittance is similar but the peak values of the emittance and the size are reduced as shown in Figure 18.

B. 1nC

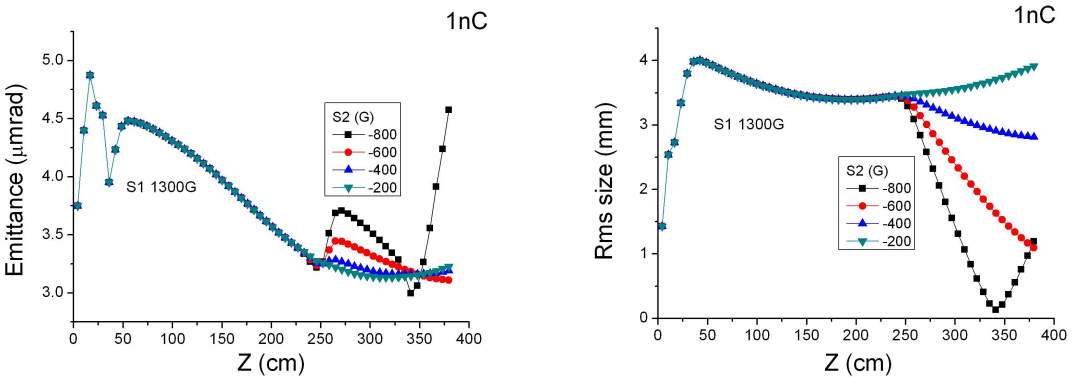

(a) (b)

FIG. 19: Evolution of (a) emittance and (b) rms size with 1nC charge.

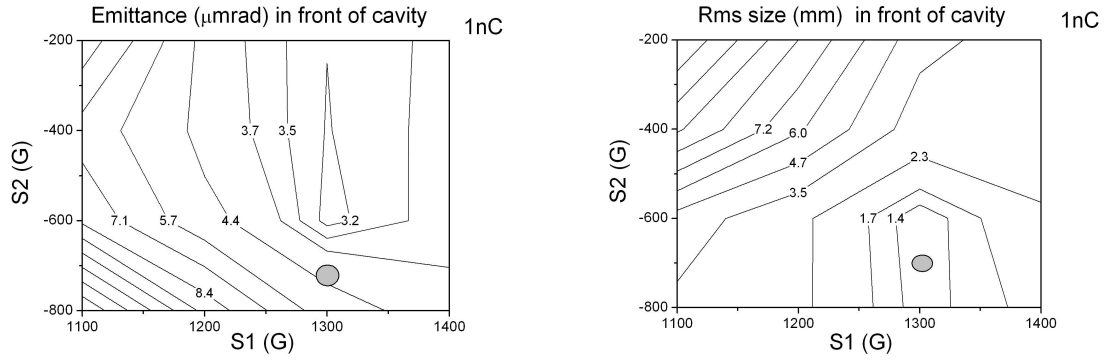

(a) (b)

FIG. 20: (a) Emittance and (b) rms size map with solenoids when the charge is 1nC.

1nC case is designed for the future undulator test. Since the charge is reduced, the expansion by the space-charge decreases. Smaller beam size can be used for smaller thermal emittance while the expansion is kept to similar level with 3.2nC case. The starting beam radius was 3.0mm in 3.2nC, and now the radius is reduced to 1.5mm which is the same as rms 0.75mm. The pulse length is 20ps. Because of the similar level of the expansion, the optimal strength of the main solenoid is similar, too. The second solenoid is placed at 2.5m. The beam size increases to 4mm and decreases to 3.5mm after the main solenoid as shown

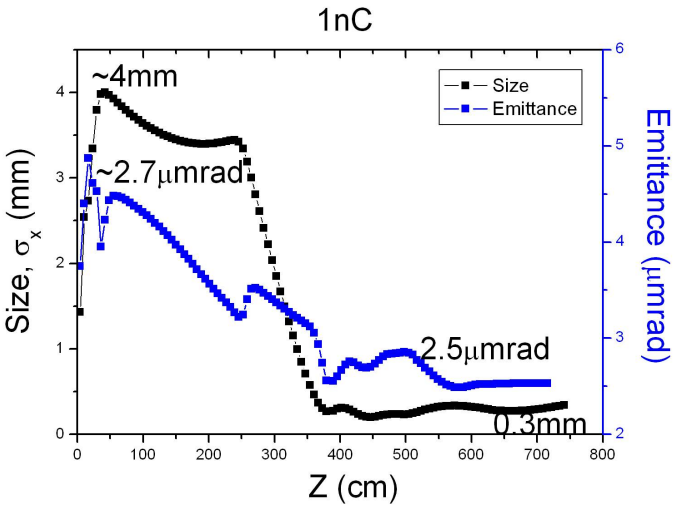

FIG. 21: Optimal case with 1nC charge.

in Figure 19(b). The second solenoid provides a kick to reduce the expansion. The beam is too focused above 600G, then the transverse emittance explodes as shown in Figure 19(a). If the strength of the solenoids are selected for the minimum size as shown in Figure 20(b), the emittance is not a minimum as shown in Figure 20(b). The optimal point will be placed near the minimums. The transverse emittance grows up to 5μmrad, then it decreases to 3.2μmrad. By taking the same strategy for the phases of the capture cavities, the optimal case is shown in Figure 21. The beam size is 0.3mm at exit, and the emittance is 2.5μmrad. This configuration is listed in Table I of the summary section.

C. 0.1nC

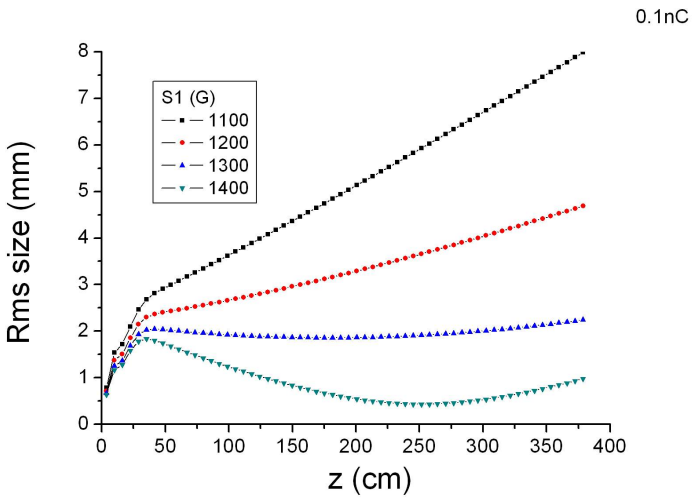

FIG. 22: Size evolution with 3.5m drift when the charge is 0.1nC.

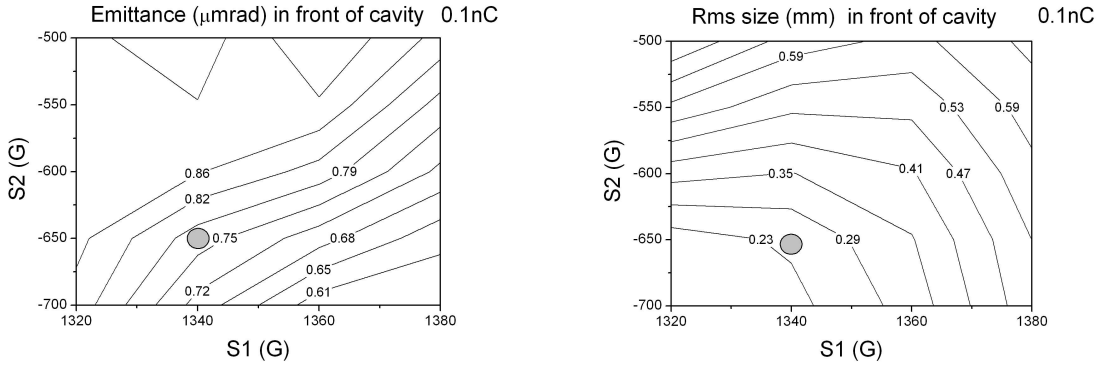

(a) (b)

FIG. 23: (a) Emittance and (b) rms size map with solenoids when the charge is 0.1nC.

0.1nC is prepared for the Compton scattering experiment. Due to smaller charge than previous cases, the bunch length is halved as 10ps and the beam radius is set to 0.5mm. Because of the shrunk dimension, the expansion shape is similar to the previous cases. The beam size with the main solenoids shown in Figure 22 after 3.5m drift, cannot be minimized. Therefore the second solenoid is necessary, too. The optimal case is chosen to have near the minimums of the size and the emittance. The set point is marked in the scan maps of the

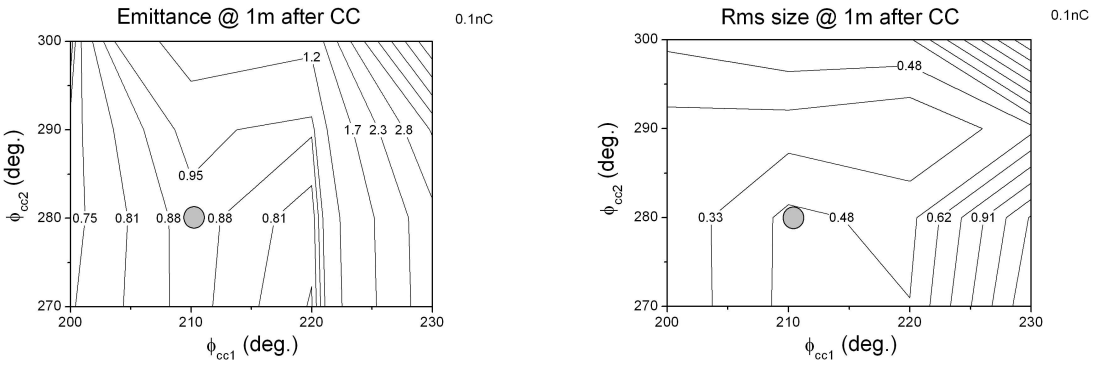

(a) (b)

FIG. 24: (a) Emittance and (b) rms size map with cavity phases when the charge is 0.1nC.

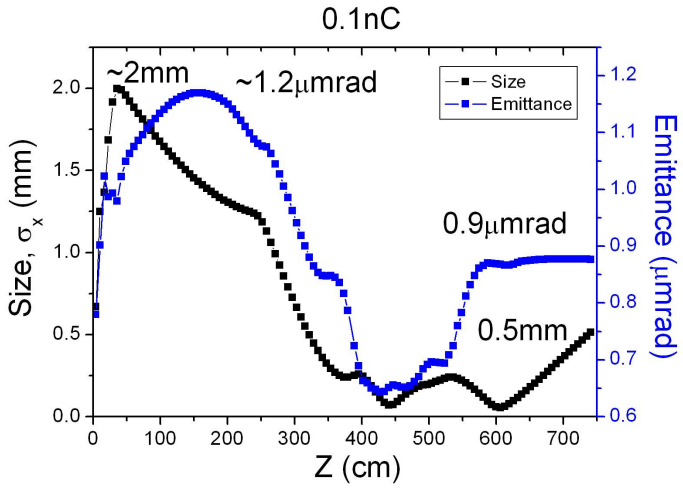

FIG. 25: Optimal case with 0.1nC charge.

solenoids as shown in Figure 23(a) and 23(b). The phases of the capture cavities are selected for the minimum emittance while the size is larger than the minimum. The working point is marked as grey filled circles in Figure reffig24. The transverse emittance is 0.9μmrad and the size is 0.5mm at exit. Their time evolution is shown in Figure 25. The maximum size is 2mm at gun exit, and the emittance reaches the maximum at 1.5m. The emittance does not increase at the entrance of the first cavity, but a kick appears at the entrance of the second cavity. It looks near the optimal but can be improved. The configuration in this level provides sub 1μmrad although it is not fully optimized.

TABLE I: Congfiguration of laser and solenoids.

Charge	Laser length	Laser radius	Laser phase	Solenoid 1	Solenoid 2
nC	ps	mm	degree	Gauss (peak)	Gauss (peak)
3.2	20	3	30	1300	750
1.0	20	1.5	30	1300	700
0.1	10	0.5	30	1340	650

TABLE II: Setup of capture cavities.

Charge	CC1 amplitude	CC1 phase	CC2 amplitude	CC2 phase
nC	MV/m	degree	MV/m	degree
3.2	12	220(-10)	12	285(-16)
1.0	12	200(-30)	12	290(-11)
0.1	12	210(-20)	12	280(-21)

V. DESIGN SUMMARY

The beam line was designed for the STF phase 2 with 3.2nC, the future undulator test with 1.0nC and the Compton scattering experiment with 0.1nC. The tracking code PARMELA was used. The round beam was assumed in this report. The beam line consists of the RF gun, the solenoids, 3.5m drift for the laser injection and the beam diagnostics, two capture cavities and followed by 1m drift. The peak field of the RF gun was fixed as 40MV/m due to 3MW maximum output power of the klystron. The average accelerating field of the capture cavities are limited as 12MV/m to avoid strong edge effect. The solenoid strengths and the cavity phases were selected for a minimal emittance at exit, in the scan maps of two variables. The configurations of the optimal cases are listed in Table I and II. The transverse emittances are 10μmrad for the 3.2nC case, 2.5μmrad for the 1.0nC case, and 0.9μmrad for the 0.1nC case. The major beam properties are listed in Table III. The beam energies after the capture cavities were about 20MeV and the energy spreads are 0.7%, 0.1% and 0.6% respectively. The beam size and the length were kept in a certain level, not fully optimized. Further optimization should be performed with some additional restrictions beyond the capture cavities.

TABLE III: Beam properties.

Charge	Emittance	Beam size	Energy	Energy spread	Length
nC	μm rad	mm	MeV	%	mm
3.2	10	2.6	21.6	0.7	2.6
1.0	2.5	0.3	20.1	0.1	2.0
0.1	0.9	0.5	21.0	0.6	0.9

VI. FURTHER STUDY

In this report, 2,000 macro-particles generated by the quasi-random were used to describe the bunch in 6-dimensional space. More macro-particles are needed for sub-ten percent error in the emittance evaluation. Besides the numerical setup, the beam-line model should be improved as the followings:

- a flat beam for ILC cavity test.
- a 4-bended chicane for the laser passage in a drift between the RF gun and the capture cavities.
- a chicane for the bunch compression.
- 6m drift after the capture cavities. Several quadrupoles magnets are included.
- the edge effect of the capture cavities with a higher accelerating field.
- the HOM generation and its effect on the beam.
- the sensitivity of each parameters and the mis-alignments.

[1] ILC Reference Design Report, ILC-Report-2007-001 (2007), http://www.linearcollider.org/cms/?pid=1000437

[2] Hitoshi Hayano, et al., "KEK-STF status", Proc. of the 4th Japanese Accelerator Society meeting, 2007.

[3] K. Flöttmann, et al., TESLA FEL-Report 1997-01 (1997).

[4] K. Hasegawa, et al., Nucl. Inst. Meth. A, vol 554, page 59-63 (2005).

[5] J. L. Coacolo, et al., TESLA FEL Report 1996-04 (1996).

[6] H. Tomizawa, et al., Proc. of FEL 2007, WEPAU01 (2007).

[7] Y.-E Sun, et al., Proc. of LINAC 2004, TUP48 (2004).

[8] F. Löhl, et al., DESY-THESIS 2005-014 (2005).

[9] W. H. Press, et al., "Numerical Recipes in C", ISBN 0-521-43108-5 (1988).

[10] S. Schreiber, et al., Proc. of EPAC 2002, TUPRI052 (2002).

[11] S. Kashiwagi, private communication.

[12] M. Ferrario, et al., TESLA TDR chap. 9 (2001).

[13] S. Schreiber, Proc. of 27th Int. FEL Conf. (2005).

[14] M. Krasilnikov, 37th ICFA Beam Dynamics Workshop Future Light Sources (2006).

[15] R. Brinkmann, et al., TESLA Technical Design Report (2001).

[16] F. Zhou, TESLA FEL-Report 1999-02 (1999).

[17] S. Schreiber, Proc. of EPAC 2004, MOPKF022 (2004).

[18] P. Castro, Proc. of EPAC 2002, MOPRI036 (2002).